

# "GENETICALLY ENGINEERED" NANOSTRUCTURE DEVICES

GERHARD KLIMECK, CARLOS H. SALAZAR-LAZARO, ADRIAN STOICA, AND  
THOMAS CWIK

Jet Propulsion Laboratory, California Institute of Technology, Pasadena, CA 91109

## ABSTRACT

Material variations on an atomic scale enable the quantum mechanical functionality of devices such as resonant tunneling diodes (RTDs), quantum well infrared photodetectors (QWIPs), quantum well lasers, and heterostructure field effect transistors (HFETs). The design and optimization of such heterostructure devices requires a detailed understanding of quantum mechanical electron transport. The Nanoelectronic Modeling Tool (NEMO) is a general-purpose quantum device design and analysis tool that addresses this problem. NEMO was combined with a parallelized genetic algorithm package (PGAPACK) to optimize structural and material parameters. The electron transport simulations presented here are based on a full band simulation, including effects of non-parabolic bands in the longitudinal and transverse directions relative to the electron transport and Hartree charge self-consistency. Two different numerical experiments that maximize the fit between experiment and simulation are presented: 1) structural variations in layer widths and doping concentrations, and 2) variations in the bulk bandstructure parameters.

## INTRODUCTION

The NASA/JPL goal to reduce payload in future space missions while increasing mission capability demands miniaturization of measurement, analytical and communication systems. Currently, typical system requirements include the detection of particular spectral lines, associated data processing, and communication of the acquired data to other subsystems. While silicon device technology dominates the commercial microprocessor and memory market, semiconductor heterostructure devices maintain their niche for light detection, light emission, and high-speed data transmission. The production of these heterostructure devices is enabled by the advancement of material growth techniques, which opened up a vast design space. The full experimental exploration of this design space is unfeasible and a reliable design tool is needed.

Military applications have similar system requirements to those listed above. Such requirements prompted a device modeling project at the Central Research Laboratory of Texas Instruments (which transferred to Raytheon Systems in 1997). NEMO was developed as a general-purpose quantum mechanics-based 1-D device design and analysis tool from 1993-97. The tool is available to US researchers by request on the NEMO web site<sup>1</sup>. NEMO is based on the non-equilibrium Green function approach, which allows a fundamentally sound inclusion of the required physics: bandstructure, scattering, and charge self-consistency. The theoretical approach is documented in references [2, 3] while some of the major simulation results are documented in references [4-6]. This paper highlights the recent work on genetic algorithm based device parameter optimization.

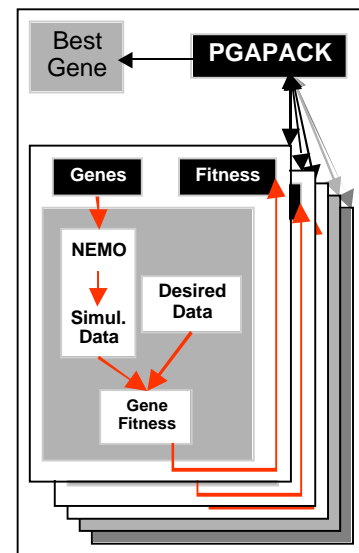


Figure 1: Architecture of a genetic algorithm-based NEMO simulation.

# QUANTUM DEVICE PARAMETER OPTIMIZATION USING GENETIC ALGORITHMS

Heterostructure device designs involve the choice of material compositions, layer thicknesses, and doping profiles. Material parameters such as band offsets, effective masses, dielectric constants etc. influence the device simulation results in addition to the structural design parameters. The full exploration of the design space using purely experimental techniques is unfeasible due to time and financial constraints. For example, it takes a well-equipped research laboratory approximately five working days<sup>7</sup> for the growth, processing and testing of a particular resonant tunneling diode design. NEMO can provide quantitative<sup>4-6</sup> current voltage characteristics (I-V's) within minutes to hours<sup>8</sup> of CPU time for a single set of device and material parameters. With this quantitative simulation capability the design parameter space can be explored expediently once an automated system for the design parameter variation is implemented. This paper presents the combination of NEMO with a parallelized genetic algorithm package (PGAPACK)<sup>9</sup> as indicated in Figure 1. The architecture lends itself to the optimization of any parameters that enter a NEMO simulation. To evaluate how good a particular parameter set is, a fitness function must be developed as discussed in the next section.

## SIMULATION TARGET AND FITNESS FUNCTION

In this work the RTD is used as a vehicle to study the effects of structural and doping variations on the electron transport. I-V's of two devices that are part of a well-behaved test matrix of experimental data published in reference [5] are used as a design target. The raw I-V data (see the example in Figure 2) contains a contact series resistance and oscillations in the negative differential resistance (NDR). The oscillation in the NDR is attributed to external circuit effects<sup>10</sup> and cannot be simulated within NEMO. The step-like feature in the NDR is cut out of the raw data to generate a "clean" set of experimental data. The contact series resistance can be estimated from the peak current of a series of nominally identical devices<sup>5</sup> with different cross sections. The voltage drop over the contact resistance can be subtracted out of the extrinsic sections.

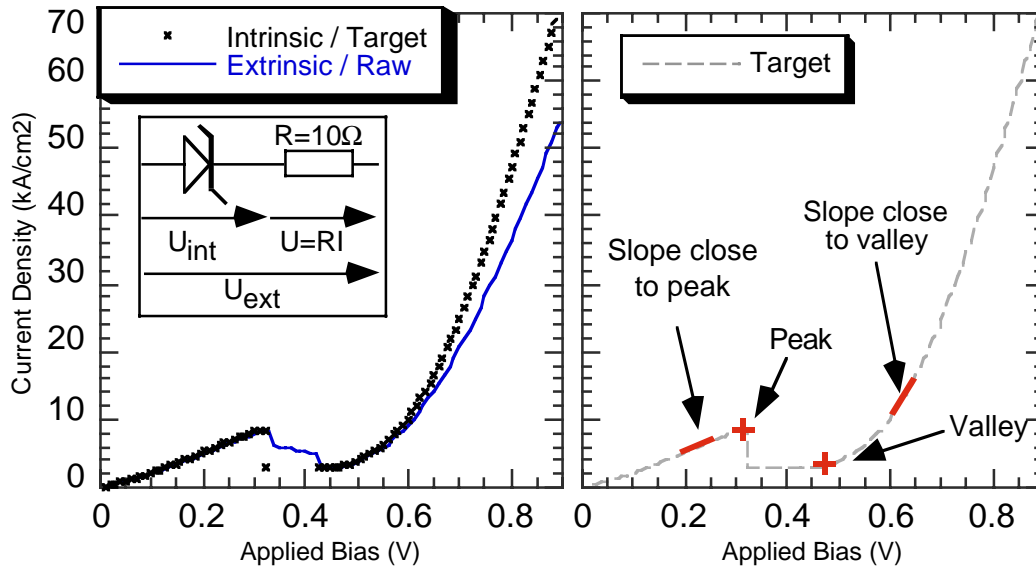


Figure 2: Generation of the target I-V characteristic of a typical resonance tunneling diode. (a) The extrinsically measured I-V (solid line) includes a series resistance and oscillations in the negative differential conductance region (0.32V-0.43V). The series resistance can be estimated from a series of devices with different cross sections. The intrinsic I-V is the target for the optimization (crosses). (b) Features that enter into the evaluation of the fitness of simulated data. Of particular interest are the peak and valley voltage and current and the slopes close to the peak and the valley.

voltage scale to yield the intrinsic voltage scale (see inset of Figure 2a)

The fitness of the simulated data is measured against such target I-V. There are four particular features that are explicitly evaluated for each simulated I-V: peak and valley current and voltage, and the slope close to the peak and the valley (see Figure 2b). Differences between the target and the simulation in these four features and the absolute and relative error for all simulated data points enter into the fitness function with a weighted average. The target fitness evaluated against itself results in a value of 1. Disagreements between simulation and target result in fitness values between 0 and 1.

## TRANSPORT MODEL

The electron transport simulations are based on a single band model, which incorporates<sup>3</sup> effects of non-parabolic bands in the longitudinal and transverse directions relative to electron transport. The model parameters are derived from a tight binding sp<sup>3</sup>s\* multiband model. This single band model captures the relevant transport physics such as complex band wrapping in the barriers and the non-parabolicity of the conduction band. The computation of the non-parabolic single band model executes about 60 times faster than the computation of the full band sp<sup>3</sup>s\* model (for structures considered here). This dramatic increase in speed allows inclusion of Hartree charge self-consistency with non-parabolicity in the transverse direction. The double integral in total energy and transverse momentum to obtain the electron density at each site *i* (Eq. (1)) is carried out explicitly<sup>2</sup> in the inner loop of the charge self-consistency. The current density is evaluated self-consistently with the electron density in the double integration.

$$n_i \propto \int k dk \int K_i(k, E) dE \quad (1)$$

$$I \propto \int k dk \int T(k, E) (f_L(E) - f_R(E)) dE \quad (2)$$

## SET-UP OF NUMERICAL EXPERIMENT

In the numerical experiment described in Figure 3, five parameters (2 doping concentrations,  $N_1$ ,  $N_2$ , and 3 thicknesses,  $T_1$ ,  $T_2$ ,  $T_3$ ) are varied within the genetic algorithm in order to achieve the best fit to an experimental I-V curve. The simulation is started from a random population of 200 parameter sets. The doping population is logarithmically distributed around the nominal values by factors of 10 ( $N_1$  [1x10<sup>17</sup>, 1x10<sup>19</sup>],  $N_2$  [1x10<sup>14</sup>, 1x10<sup>16</sup>]). The layer thickness population is uniformly distributed around the nominal value by 10 monolayers ( $T_1$  [1, 17] for device 1,  $T_1$  [10, 30] for device 2,  $T_2, T_3$  [6, 26]). In each generation 63 of the worst genes<sup>11</sup> are dropped out of the population and new genes are generated<sup>9</sup> from the rest by mutation and crossover. Mutation allows the parameters to leave the original parameter range.

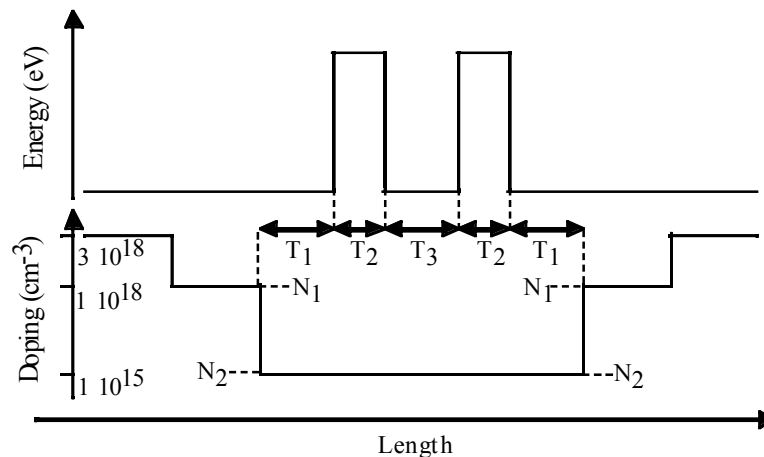


Figure 3 Conduction band edge and doping profile of a typical resonant tunneling diode. The central device region is typically undoped. The low doped spacer thickness, the barrier thicknesses and the well thickness are labeled  $T_1$ ,  $T_2$ , and  $T_3$ , respectively. The low spacer doping and the central device doping are labeled  $N_1$  and  $N_2$ ,

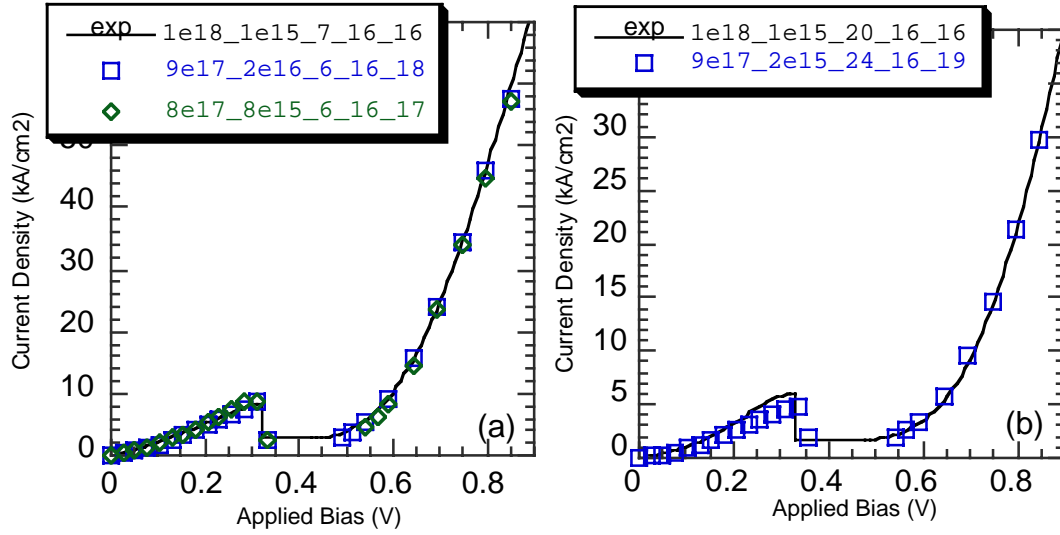


Figure 4: Current voltage characteristics of two different InGaAs/InAlAs resonant tunneling diodes. The nominal structures have barrier ( $T_2$ ) and well ( $T_3$ ) thicknesses of 16 monolayers (ml), and doping a doping profile of  $10^{18} \text{ cm}^{-3}$  ( $N_1$ ) and  $10^{15} \text{ cm}^{-3}$  ( $N_2$ ). The devices (a) and (b) differ nominally in their no-doping spacer thicknesses ( $T_1$ ) of 7 and 20 ml, respectively. The solid lines show experimental data published in reference [5], where the noise in the valley current region was eliminated. The curves are labeled by the 5 parameters  $N1\_N2\_T1\_T2\_T3$ .

## SIMULATION RESULTS

Two I-V's from slightly different structures serve as a target of the genetic algorithm optimization. Both structures were specified to the grower to have 16 monolayers (ml) of barriers ( $T_2$ ) and well ( $T_3$ ), no intentional doping in the central device ( $N_2=1 \times 10^{15} \text{ cm}^{-3}$ ),  $N_1=1 \times 10^{18} \text{ cm}^{-3}$  doping in the low doping spacers, and  $3 \times 10^{18} \text{ cm}^{-3}$  in the high doping contacts (see Figure 3). The nominally only difference in the two devices is in the no-doping spacer length  $T_1$  of 7 vs. 20 ml. The simulation is started from the random populations as described in the previous section. The genetic algorithm converges for both I-V's to the nominal structure values, well within the experimental uncertainty as shown in Figure 4. Again it is found that the well widths must be increased in the simulation by a few monolayers versus the nominal values to achieve the best agreement with experimental data<sup>5</sup>. Different relative weights will result in different "optimal" structures as shown in Figure 4b.

## FUTURE WORK

This work is the first step to integrate NEMO within a high performance parallel computational environment. A desired curve can now be entered as the target of the simulation and the genetic algorithm is expected to obtain the optimal parameter set. Future work will utilize this method to analyze the vast material and structure parameter space. It is planned to evaluate other optimization techniques such as simulated annealing and directive approaches as well. These optimization techniques will be made available within a graphical user interface which enables the selection of parameters to be varied, the setting of parameter ranges and the setting of optimization parameters, such as population sizes, and mutation and crossover rules.

## SUMMARY

We present the first NEMO simulations driven by a genetic algorithm to optimize parameters such as layer thicknesses and doping profiles. The convergence of the initially

random population of devices to experimental specified device parameters is demonstrated for two different devices. The transport simulation are performed within a novel non-parabolic single band model which is derived from a more complete sp<sup>3</sup>s\* tight binding model. This single band model captures the relevant transport physics such as complex band wrapping in the barriers and the non-parabolicity of the conduction band in the longitudinal and transverse transport direction. These simulations are performed for the first time in Hartree charge self-consistency.

#### Acknowledgement

The research described in this paper was carried out by the Jet Propulsion Laboratory, California Institute of Technology, under a contract with the National Aeronautics and Space Administration.

#### BIBLIOGRAPHY

1. NEMO, Nanoelectronic Modeling, in <http://www.raytheon.com/rtis/nemo/>.
2. R. Lake et al., J. Appl. Phys., **81**(12), 7845 (1997).
3. R. Lake et al., phys. stat. sol. (b), **204**, 354 (1997).
4. G. Klimeck et al., Appl. Phys. Lett., **67**(17), 2539 (1995).
5. G. Klimeck et al., IEEE DRC, 1997: p. 92.
6. R. C. Bowen et al., J. Appl. Phys., **81**, 3207 (1997).
7. A. C. Seabaugh, Texas Instruments, private communication, 1997.
8. The actual CPU time needed for a single I-V simulation depends strongly on the choice of material systems, bandstructure models, temperature scattering models, and bias points. The individual I-V characteristics presented here take about 30 minutes to compute on a single 200MHz R10000 CPU of an SGI Origin.
9. D. Levine, <http://www-unix.mcs.anl.gov/~levine/PGAPACK/index.html>, Parallel Genetic Algorithm Library.
10. J. N. Schulman, Second Workshop on Characterization, Future Opportunities and Applications of 6.1Å III-V Semiconductors, Aug. 24-26, 1998, Naval Research Laboratory, Washington, DC, <http://estd-www.nrl.navy.mil/code6870/code6870.html>. H. C. Liu, J. Appl. Phys. **64**, 4792 (1988). . H. C. Liu, J. Appl. Phys. **53**, 485 (1988).
11. LAPACK is implemented with MPI where N-1 of N processors are slaves to one master processor. The master takes care of the collection of data from the slaves. In a cluster of 64 CPU's we therefore renew only 63 genes in every generation.